Hybridization approach to in-line and off-axis (electron) holography for superior resolution and phase sensitivity

C. Ozsoy Keskinbora[1], C. B. Boothroyd[2], R.E. Dunin-Borkowski[2], P.A. van Aken[1], C.T. Koch[3]

[1] Stuttgart Center for Electron Microscopy, Max Planck Institute for Intelligent Systems, Heisenbergstr. 3, 70569 Stuttgart, Germany

[2] Ernst Ruska-Centre for Microscopy and Spectroscopy with Electrons and Peter Grünberg Institute, Forschungszentrum Jülich, 52425 Jülich, Germany

[3] Institute for Experimental Physics, Ulm University, 89069 Ulm, Germany

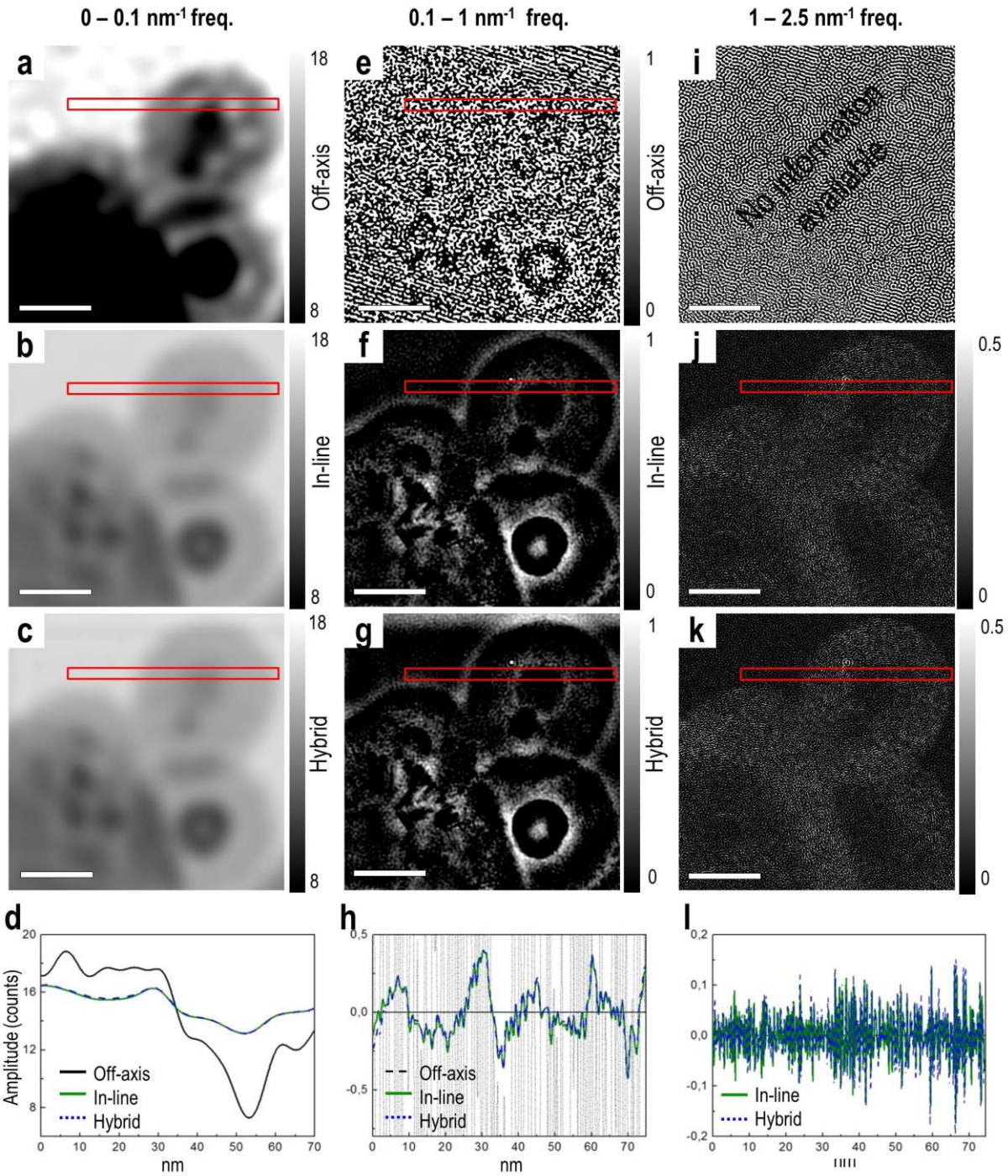

Supplementary Figure 1: Band-pass-filtered amplitude images for frequency ranges of (a, b, c) 0–0.1 nm^{-1}; (e, f, g) 0.1–1 nm^{-1}; (i, j, k) 1–2.5 nm^{-1}. Top row: off axis; middle row: in-line; bottom row: hybrid method. Line profiles generated from the boxes marked in red are shown in (d), (h) and (i). Scale bar, 20 nm.

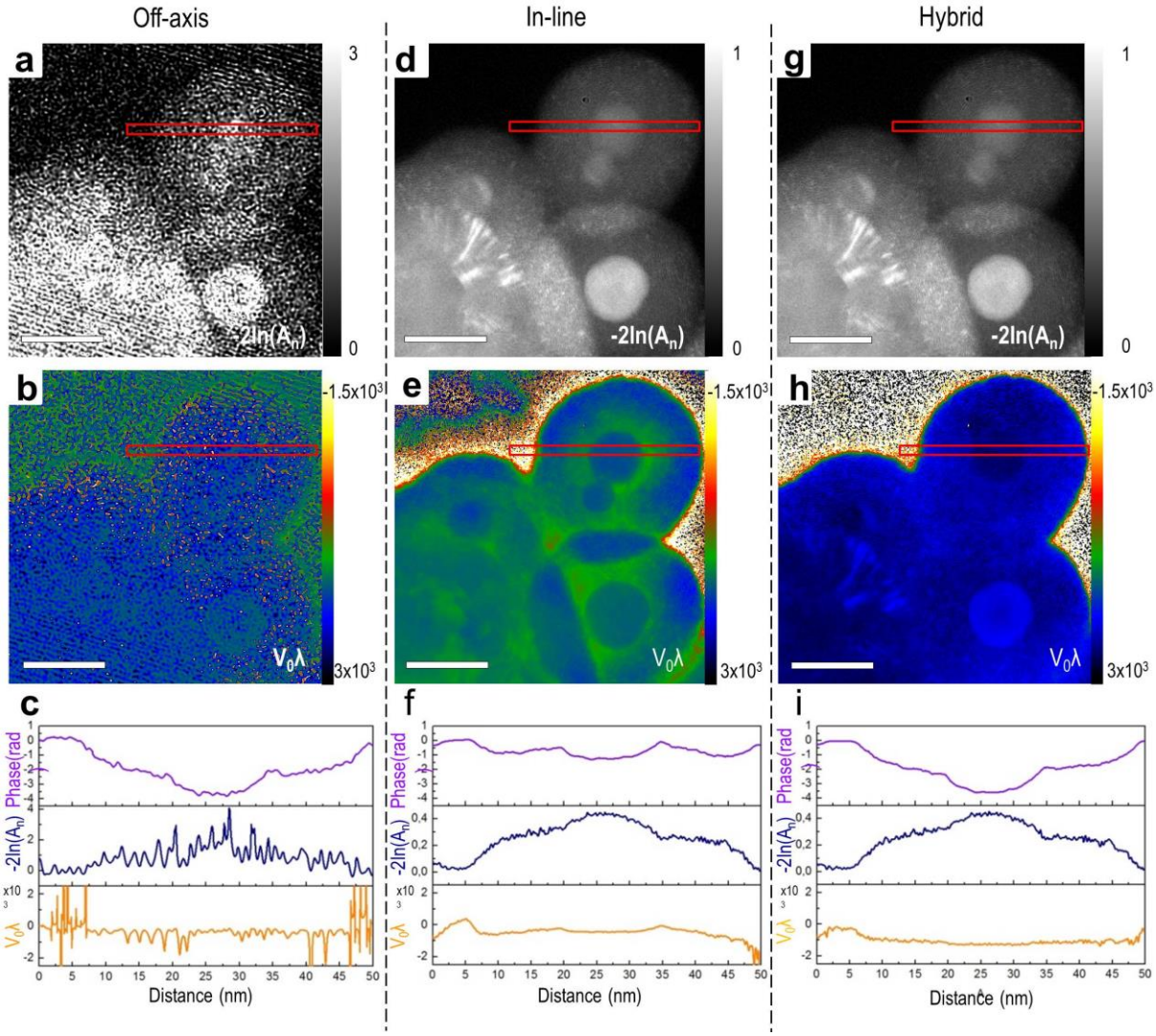

Supplementary Figure 2: Thickness independent mena inner potential maps: Top row (a,d,g): The inverted logarithm of the reconstructed amplitudes (specifically $-2\ln(A_n)$) calculated for the off-axis, in-line and hybrid methods. Middle row (b,e,h): thickness-independent $V_0\lambda$[1,2] images calculated for the of off-axis, in-line and hybrid methods. Profiles extracted from the boxes marked in red are shown in (c), (f) and (i). Scale bar, 20 nm.

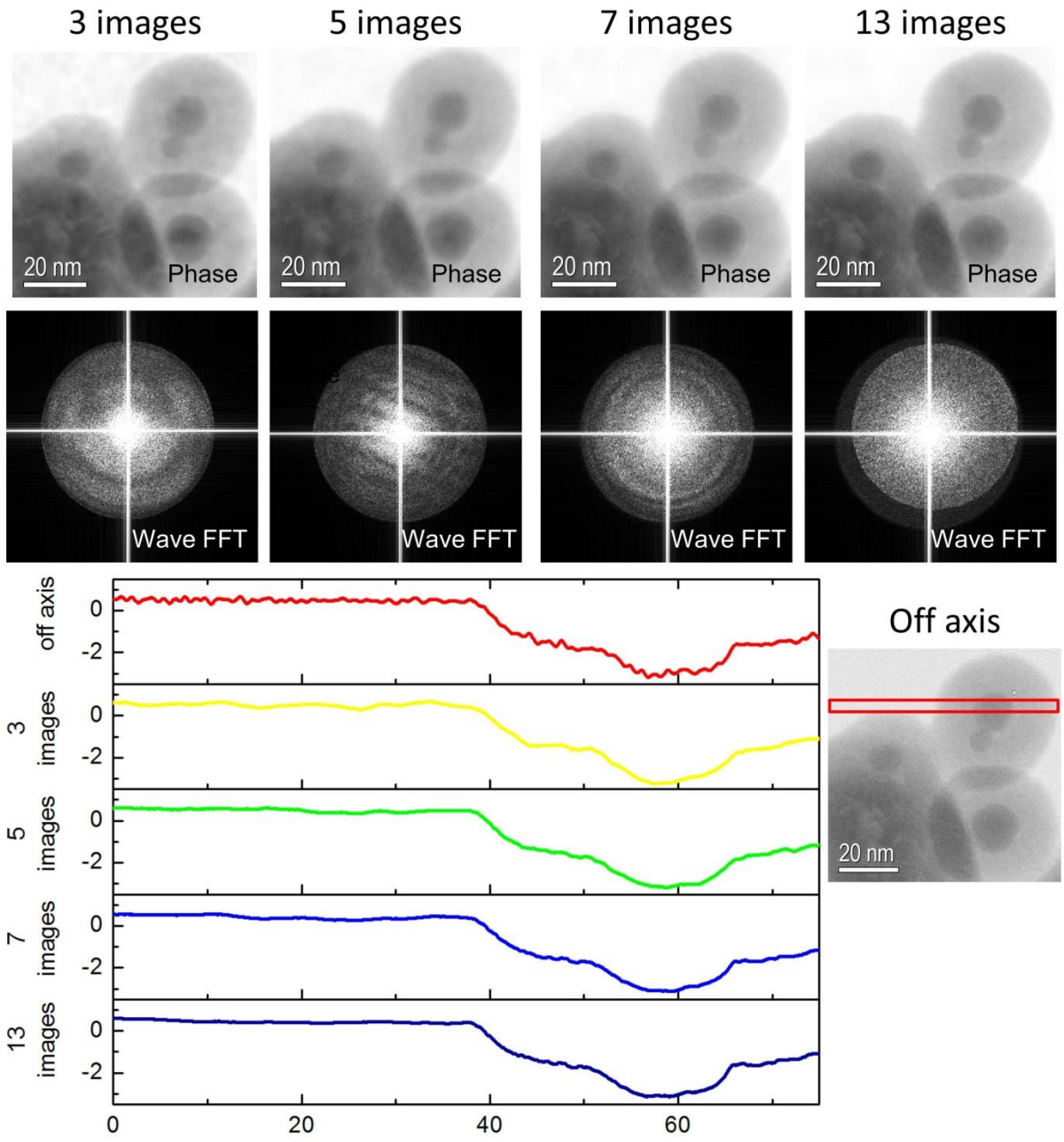

Supplementary Figure 3: Illustration of the effect of the number of defocus steps used for the reconstruction. Top row: phase images reconstructed using the different numbers of defocus images indicated. Middle row: Fourier transforms of the images in the top row. Bottom row: phase profiles obtained from the region marked in red in the off-axis phase image shown on the right.

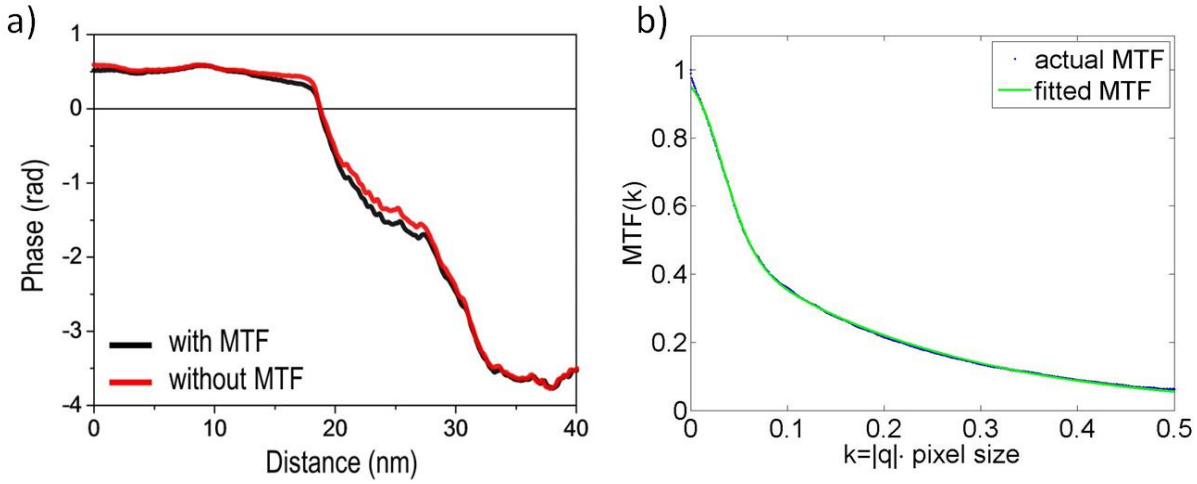

Supplementary Figure 4: The effects of MTF a) Illustration of the effect on the phase profile of taking the MTF of the CCD camera into account. b) MTF of the CCD camera being used for this experiment. In order to smoothen the MTF for use in the reconstruction the following equation was fitted to it: $MTF(k) = 0.5559 \cdot \exp(-4.6362 \cdot k) + 0.3925 \cdot \exp(-458.2232 \cdot k^2)$ [3]. The abscissa and **k** in this expression are both the normalized spatial frequency, i.e. the spatial frequency |**q**| multiplied by the detector pixel size, so that $\mathbf{k}_{Nyquist} = 0.5$. The MTF data measured for the 10 lowest values of *k* were not included in the fit.

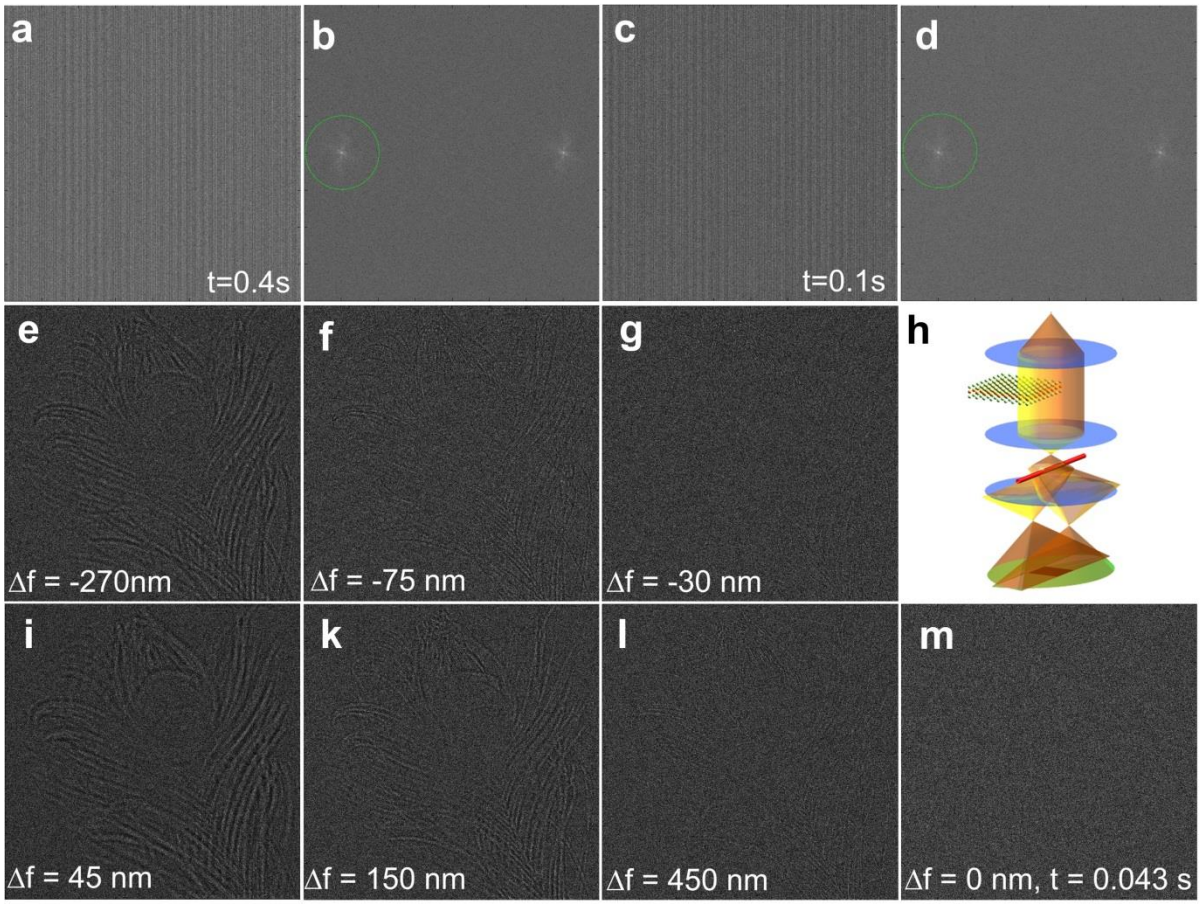

Supplementary Figure 5: The effect of exposure time: Simulated 80 kV off-axis and inline holography data used to recover the phase images shown in Fig. 4. Poisson noise has been added in order to simulate the effect of finite exposure time. Round illumination (ε=1), a source brightness of $\beta = 2 \cdot 10^8$ Acm^{-2}sr^{-1}, a pixel size of 0.1 nm, and a field of view of 80 nm have been assumed. (a) Off-axis hologram simulated for an exposure time of 0.4 s. The shear distance x_{Shear} was equal to the field of view, and an optimized illumination semi-convergence angle of $\alpha = \lambda/(\sqrt{2}\,\pi x_{Shear})$ = 11.7µrad was assumed [4]. Fresnel fringes due to the biprism have not been simulated. (b) Fourier transform of (a). (c) and (d) Off-axis hologram and FFT for an exposure time of 0.1 s. The green circles in (b) and (d) indicate the size and position of the numerical aperture used to reconstruct the wavefunction. (e), (f), (g), (i), (k), (l), and (m) show the inline holograms simulated for the indicated planes of focus and exposure times of 0.043 s, adding up to a total of 0.3 s for the complete series. The illumination conditions were chosen identical to those used for the off-axis simulation. (h) Round illumination (ε=1) and a high spatial coherence (the small α specified above) were assumed, in agreement with the experiment.

Supplementary References

1. Gajdardziska-Josifovska, M. & McCartney, M. R. Elimination of thickness dependence from medium resolution electron holograms. *Ultramicroscopy* **53,** 291–296 (1994).
2. McCartney, M. R. & Gajdardziska-Josifovska, M. Absolute measurement of normalized thickness, t/λi, from off-axis electron holography. *Ultramicroscopy* **53,** 283–289 (1994).
3. Van den Broek, W., Van Aert, S. and Van Dyck, D. Fully Automated Measurement of the Modulation Transfer Function of Charge-Coupled Devices above the Nyquist Frequency. *Microscopy and Microanalysis* **18**, 336-342 (2012)
4. A. Harscher, H. Lichte, Experimental study of amplitude and phase detection limits in electron holography, Ultramicroscopy **64**, 57–66 (1996)